

## Title

Techno-economic assessment of renewable hydrogen production and the influence of grid participation

---

## Abstract

Large-scale hydrogen production facilities will be required to supply the chemical energy demand of certain industries in the future. The case for such production plants based on individual adapted PV and wind farms has been addressed in several studies. However, most studies focus on an island solution of the evaluated plant and therefore, do not allow grid assistance which significantly reduce the installed capacity of the corresponding units. To address this issue, we developed a tool with a linear programming approach to evaluate any location around the world for its renewable hydrogen production costs and the influence on the plant layout depending on its interaction with the grid. A detailed techno-economic evaluation has been performed for five locations where hydrogen production costs in the range of 4 – 6 €<sub>2020</sub>/kg have been retrieved. Furthermore, it is shown that with perspective cost data the costs can further be reduced to 2.50 €<sub>2020</sub>/kg.

---

# 1. Introduction

The usage of fossil based primary energy carriers has caused an increase in the concentration of CO<sub>2</sub> and other greenhouse gases (GHG) in earth's atmosphere resulting in global warming and the climate crisis. While there are political instruments implemented around the globe to reduce these emissions, with current measures mankind will most likely fail the goal of the COP21 Paris Agreement limiting global warming to "well below" 2 °C (1, 2). In order to reach the 1.5 °C goal, a rapid electrification of end-use applications, especially in the heating and transportation sectors is required (1). But there are sectors where a direct electrification is not feasible e.g., the steel industry, aviation or shipping. For these sectors hydrogen and hydrogen-based synthetic fuels will have to replace fossil chemical energy carriers in order to reach the climate goals (1). This issue is addressed by an enormous increase in global funding for research activities and first demonstration projects regarding all aspects of a global hydrogen economy like the production, distribution, and utilization (directly and via hydrogen-based fuels) (3-5). For the case of Germany, the hydrogen demand for the year 2030 is predicted to be in the range of 90 – 110 TWh, of which about 14 TWh can be produced domestically (6). Hydrogen import options might prevail in the near future while its origin is not determined yet. Countries like Chile and Australia recently got a lot of attention for their high potential to produce renewable energy (RE), such locations are called "sweet spots". A transparent techno-economic based rating of different locations is required and the first step to develop a hydrogen import options map. Further social aspects, e.g. considering the local population and its own development goals, must get addressed as well. The increase of RE-capacity has to be carried out under a fair development partnership (7).

Only countries and regions with a clear climate-protection roadmap, e.g. electrifying their own energy system, should be considered to provide hydrogen or hydrogen-based fuels to the rest of the world.

If a certain sweet spot is selected to build a hydrogen production plant from local "excess" RE, the layout of the whole plant must be individually designed to the local conditions in order to achieve high capacity factors of the RE sources and due to the high required investments (7). Furthermore, the intermittency of the renewable power supply and its implications on the consecutive hydrogen conversion step needs to be considered. Cryogenic liquefactions as well as the Fischer-Tropsch synthesis, as an exemplary PtX process, are usually designed to run in a stationary mode; even though recent studies focus on the dynamic behavior of these processes (8, 9). Load changes will considerably reduce the production rate, they can lead to increased thermal stress resulting in higher maintenance costs as well as challenges in the design of the process. In this study a hydrogen production plant with its own RE sources is designed, so that a consecutive conversion step gets supplied with a constant flow of hydrogen. Consequently, storage devices for electricity and hydrogen will be required for such a plant.

Several studies have examined the production costs for green hydrogen. In order to take the fluctuating renewable energy supply into account, a dynamic simulation with an hourly temporal resolution is usually considered. Mallapragada et al. (10) assessed the levelized cost of hydrogen (LCOH<sub>2</sub>) for the year 2030 for solar energy (PV) based plants with a continuous hydrogen supply of 100 t/d in the US. An “island solution” was considered for every plant, meaning no relevant external mass or energy flows, except the water input and hydrogen output are considered. They identified a set of locations around the US where the LCOH<sub>2</sub> were as low as 2.5 \$/kg with a plant availability of 95 % if a salt cavern could be used as intermediate hydrogen storage. Schnülle et al. (11) assessed the current LCOH<sub>2</sub> for northern Germany based on PV, onshore, and offshore windfarms, also focusing on island solutions in their business cases. In their study, a direct link from the power source to the electrolysis is considered, mainly due to the German energy law to avoid higher costs from grid fees and taxes. The minimum costs amount to 4.33 €/kg<sub>H<sub>2</sub></sub> for the case with an alkaline electrolysis and electricity from a fully depreciated onshore wind farm (11). Vartiainen et al. (12), while also considering an island solution with an electrolyzer capacity of 100 MW<sub>el</sub>, estimated the PV based LCOH<sub>2</sub> for 10 locations for current costs as well as perspective costs up until the year 2050. Their results indicate that the LCOH<sub>2</sub> in the year 2050 are lower than the current LCOH<sub>2</sub> based on methane steam reforming, 0.30 - 0.84 €/kg compared to roughly 1.70 €/kg for every location considered (13). The year 2050 is also the reference year of the “PtX-Atlas” published by Pfennig et. al (14). They focused on the LCOH<sub>2</sub> of liquid hydrogen in coastal locations and retrieved values of 1.92 – 4.59 €/kg.

In summary, a lot of research activity has been going on regarding the assessment of hydrogen production based on renewable energy like wind and PV and for island solutions, as can be seen in Table 1. Large-scale hydrogen production plants will interact with the local electric grid, even if they have their own RE sources. In this study, its implications on every step along the production chain will be evaluated and thoroughly discussed. With the participation of the local grid, the hydrogen production costs can be further reduced by omitting the demand for storage equipment to a certain extent. Furthermore, land use and the resulting ecological footprint might be reduced if the installed capacities of the plant can also be decreased.

Table 1: Levelized costs of hydrogen - Selection of current and perspective cost predictions

Author	Reference year	RE supply	Location considered	LCOH <sub>2</sub>
Schnülle (11)	2020	Wind & PV	Northern Germany	4.33 – 12.38 €/kg
Vartiainen (12)	2020	PV	Various (focus on high PV potential)	0.93 – 2.16 €/kg
Vartiainen (12)	2030	PV	Various (focus on high PV potential)	0.60 – 1.44 €/kg
Mallapragada (10)	2030	PV	USA (10 most favorable sites)	1.98 – 4.00 \$/kg
Pfennig (14)	2050	Wind & PV	Various (global PtX-Atlas)	1.92 – 4.59 €/kg (liquid)

The aim of this study is a reproducible and transparent assessment of hydrogen production plants designed to minimize each site-specific cost for a constant hydrogen supply including potential grid support. Several sweet spots around the globe are evaluated to consider different climate conditions. Grid assistance leads to the fact that the produced hydrogen will not be 100 % renewable, but it might be beneficial from a technical, economic and even ecological point of view. This relationship between partial electric grid support and the optimal dimensioning of the unit operations is the focus of this study. The basic outline of the hydrogen supply plant is depicted in Figure 1. The consumer might be a liquefaction plant for green hydrogen export or any other PtX-plant.

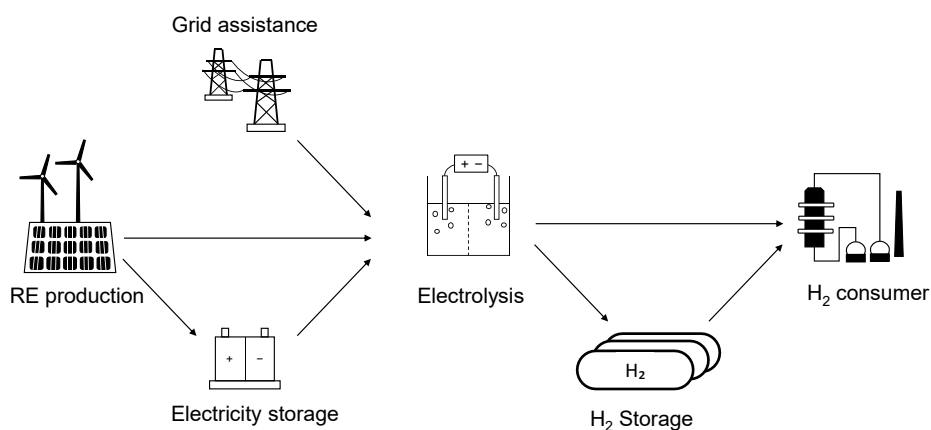


Figure 1: Basic process layout of a hydrogen production plant

## 2. Methodology of techno-economic evaluation

### 2.1. Definition of the case study

In this study, the layout of a plant is evaluated that continuously supplies an undefined downstream processing plant with hydrogen. To consider different climate conditions, 5 sweet spots around the globe are evaluated. First, a **base case [BC]** is evaluated to retrieve the currently achievable minimal LCOH<sub>2</sub>, which will be reported in €<sub>2020</sub>/kg<sub>H<sub>2</sub></sub>. The base case considers the current technical and economic progress and an “island solution” as reference frame. Then, different scenarios are evaluated; to mimic downtime periods of the downstream plant, the **downtime case [DT]** is considered where no hydrogen is delivered to the downstream processing plant for a consecutive time of 760 hours. This case is evaluated to see, if purposely overlapping schedulable maintenance works with periods of low RE production potential will be beneficial for the LCOH<sub>2</sub>, since hydrogen processing plants have usually 8'000 operating hours per year (15). In the cases **G-10** and **G-25** no downtime is considered but the influence on the plant layout is determined when a certain amount of power can be drawn from the electric grid. For the G-10 case, the electric power drawn from the grid is enough to meet 10 % of the required hydrogen flow and 25 % in the G-25 case, respectively. All cases are listed in Table 2. Additionally, in a sensitivity analysis the future reduction potential of LCOH<sub>2</sub> will be outlined by using cost decline predictions. In the sensitivity analysis cost predictions for photovoltaic (PV) cells and electrolyzers are considered, for further details see subchapter 3.1.1 and 3.3. The total annual hydrogen mass flow is taken from a previous study and amounts to 225'500 t/a (16). This is equivalent to 10 % of the minimum hydrogen import demand in the year 2030 according to the German hydrogen strategy (6) and corresponds to 25.74 t<sub>H<sub>2</sub></sub>/h and a power output of 858 MW<sub>H<sub>2</sub>, LHV</sub>. A mass flow in this order of magnitude exceeds the limits of a scale up approach and requires numbering up of the individual process units. This justifies the linear programming approach introduced in subchapter 2.2 that is used to determine the minimal LCOH<sub>2</sub> for every location and scenario. Since the hourly mass flow will not be adapted, the annual mass flow is reduced to 205'936 t in the downtime case.

Table 2: Cases evaluated in the study

Case	Adaptation to base case
Base case - [BC]	-
Downtime case - [DT]	Downtime of 760 hours of the downstream plant is considered – evaluation as island system
Grid connection - [G-10]	Grid supply can meet 10 % of the required H <sub>2</sub> flow (2.57 t/h)
Grid connection - [G-25]	Grid supply can meet 25 % of the required H <sub>2</sub> flow (6.48 t/h)
Sensitivity - S1	Sensitivity analysis regarding PV costs
Sensitivity - S2	Sensitivity analysis regarding electrolyzer data
Sensitivity - S3	Sensitivity analysis regarding PV and electrolyzer data

As already stated, one year with a temporal resolution of one hour is considered for the dynamic simulation. For the evaluation, discrete mass and energy packages are transferred in between the unit operations of the plant, giving it a pseudo-continuous appearance. An exemplary temporal course and intermediate results are given in chapter S.1.2 in the supplementary information. RE is supplied via wind turbines and PV panels depending on their availability, which is determined from weather data from the individual location. Electric energy is either stored for later use or directly transferred to the electrolysis unit, which can either be a proton exchange membrane (PEM) or alkaline electrolysis. The produced hydrogen is transferred to the consumer or a hydrogen storage unit. The total mass flow to the consumer, meaning the mass flow from the electrolysis unit plus the flow from the storage unit, must be constant for every hour of the year. The whole plant is designed to obtain the lowest LCOH<sub>2</sub> achievable. Excess electric energy gets curtailed. If a storage unit is considered, it has the same loading level at the start and the end of the evaluated year. Meaning it can have a loading level of 47 % at the beginning but then the loading level at the end of the evaluated year must also be at 47 %. There are no upper limits regarding the installed capacities of the unit operations. Relevant data of the considered units can be found in chapter 3 and are summarized in the supplementary information. Transmission and transformation losses of electric energy are neglected. Table 3 lists the basic input values of the scenarios.

Table 3: General input values for the techno-economic assessments

	<b>Unit</b>	<b>Value</b>	<b>Source</b>
Hydrogen flow	t/h	25.74	Assumption, based on (16)
Depreciation time	a	20	Assumption, based on (15)
Weighted Average Cost of Capital (WACC) - OECD countries	-	5 %	(17)
WACC – non-OECD countries	-	7.5 %	(17)

## 2.2. Methodology of the techno-economic evaluation

The methodology of the evaluation is based on a previous study focusing on techno-economic assessments (TEA) of chemical production plants and is extended to PV and wind farms (18). Fixed capital investment (FCI) and partly the operating costs (OPEX) are estimated by using the factor method. The factors to estimate the FCI, so called “Lang-factors<sup>1</sup>”, can be found in the supplementary information (20). Remaining OPEX arise from participating with the electric grid and labor costs. With the given input data from chapter 3, specific annual costs  $C_i$ . (see Equation 1) are determined and adjusted to every location.

In order to determine the plant layout with the lowest LCOH<sub>2</sub>, a tool has been developed in using Py-Charm 2021.2 and employing the Gurobi solver (21). The underlying mathematical model determines the lowest LCOH<sub>2</sub> by minimizing the *objective function* (Equation 1) with a linear programming approach i.e., the specific annual costs  $C_i$  are independent of the corresponding installed capacity:

Equation 1: Objective function of the mathematical model

$$C_{Total} = C_{PV} \cdot x_1 + C_{Wind} \cdot x_2 + \sum_{Bat} C_{Battery} \cdot x_{3,bat} + C_{Elec} \cdot x_4 + C_{Comp} \cdot x_5 + C_{C-St} \cdot x_6 + C(h)_{Grid} \sum_{h=1}^{8760} E_{Grid,h}$$

The *decision variables* ( $x_1 - x_6$ ) of the objective function are equivalent to the required installed capacities of the corresponding units. These are the variables the solver is adapting to find the lowest LCOH<sub>2</sub>. A set of *constraints*, i.e., boundary conditions is defined by linear equations which describe all flows, conversions, efficiencies and losses of the entire hydrogen production plant. An exemplary constraint is the requirement of the constant hydrogen flow, i.e., the mass flow from the storage unit plus from the electrolyzer, as shown in Figure 1, must be equal to 25.74 t/h. Details and equations of the mathematical model like the whole set of *constraints* can be found in chapter S.1 of the supplementary information.

In addition to the LCOH<sub>2</sub>, useful intermediate results like the levelized costs of electricity (LCOE) or the capacity utilization factor (CUF) of the PV and wind farms are obtained. The dynamic behavior of the individual units and the storage systems of the plant along the year are also part of the results. However, given that the mathematical model works with the weather data of the entire year instantaneously, it inherently features “perfect foresight”. This means for example, that the

---

<sup>1</sup>: First introduced by Lang, the “Lang” factor is the ratio between the costs of an equipment that has been fully installed, designed incl. cost for building, construction etc. compared to its sole procurement costs from a vendor. For fluid processing plants the “Lang” factor equals 5

19. Peters MS, Timmerhaus KD, West RE. Plant design and economics for chemical engineers: McGraw-Hill New York; 2003.

model knows perfectly when and how much energy is required or needs to be stored to compensate for a time of scarcity in the future, operating in the leanest way. In a more realistic scenario, storage systems might be kept as full as possible during a certain season. This would result in a higher CUF of the PV and wind farms, but also in a greater loss of energy due to possible self-discharge of the storage systems. The schematic flowchart with the corresponding input and exemplary output parameters is depicted in Figure 2.

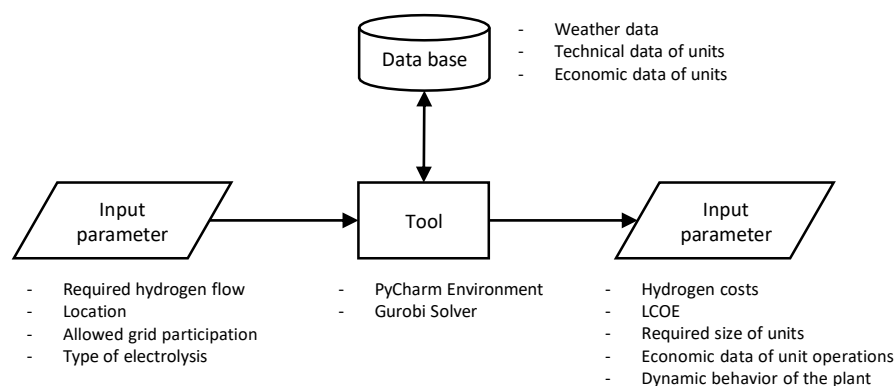


Figure 2: Schematic flow chart of the developed tool

### 2.3. Example locations for the evaluation

5 locations around the globe are evaluated. Since the influence of the grid is also evaluated, only countries with a stable grid are considered. The locations are handpicked and selected on an emphasis of high potential for wind and solar energy (22, 23). Some of the locations are already considered for large-scale renewable energy generation or PtX-projects (24-27). Table 4 lists the location considered and the corresponding coordinates for which the weather data has been retrieved. Different tilt angles for the PV panels are considered, depending on the latitude of the location, to increase the energetic output. The angles are determined by the method of Chinchilla et al. (28).

Table 4: Example locations considered for the evaluation

Location	Coordinates	PV tilt angle	Grid energy costs [€ <sub>2020</sub> /MWh]
Pampa Anita, Chile	-24.928, -69.740	24°	92.86 (29, 30)
Punta Arenas, Chile	-53.175, -70.943	39°	92.86
Sakaka, Saudi Arabia	29.744, 40.095	27°	41.96 (31, 32)
Almeria, Spain	37.093, -2.357	32°	70.50 (33)
Northampton, Australia	-28.352, 114.630	26°	197.95 (34, 35)



### **3. Unit operations of the hydrogen production plant**

In this section, the relevant aspects of the unit operations considered for a process plant, as it is depicted in Figure 1, are described.

#### **3.1. Renewable energy supply**

The availability of solar and wind energy is determined by the local and temporal weather conditions. To consider different locations, publicly available data of the weather conditions with 2019 as the reference year and a local resolution of  $0.5^\circ \times 0.625^\circ$  is used (36-38). This is equivalent to 55.6 km x 63.02 km in Pampa Anita, the location closest to the equator, and 55.6 km x 41.65 km in Punta Arenas, the location furthest away from the equator. Data for utility-scale PV and onshore wind farms are taken from (17).

##### **3.1.1. Solar energy supply**

The input variable for the determination of PV power supply is the sum of direct and diffuse solar irradiance. For simplicity reasons, all PV panels have the same orientation at a certain location and no tracking is considered. Cost data for the investment as well as operating and maintenance (O&M) of utility-scale PV farms in the corresponding countries are taken from a study published by IRENA (17). Since installed costs are given, no Lang-factors are required. Based on the efficiency, which is considered to be 20.3 % (39), the required area of PV panels is estimated. Degradation of the solar panels is neglected. Labor demand amounts to 46.33 full time equivalent (FTE) for each GW of installed PV capacity (27). For the sensitivity analysis S1 and S3, fixed costs for utility-scale PV with 100 €<sub>2020</sub>/m<sup>2</sup> are assumed. The translated values to USD<sub>2020</sub>/kW as well as all values for the solar energy supply are given in Table S.6 and S.7 of the supplementary information.

##### **3.1.2. Wind energy supply**

Local wind speed is the input variable to estimate the wind power supply. The used weather data give the average wind speed for a reference height of 80 m above the ground. For wind turbines with a different hub height, the wind speed is adapted by the power-law approach with an exponent of 1/7, which is commonly used for smooth terrain on land (40). Two different wind turbines are considered. Technical data from the model V112-3.45 MW<sup>®</sup> by Vestas is used for wind turbine I (41, 42). For wind turbine II the model GE 2.5<sup>®</sup> by General Electric is considered (43). Power curves of both turbines are shown in Figure 3. Both wind turbines have a cut-out wind speed of 25 m/s.

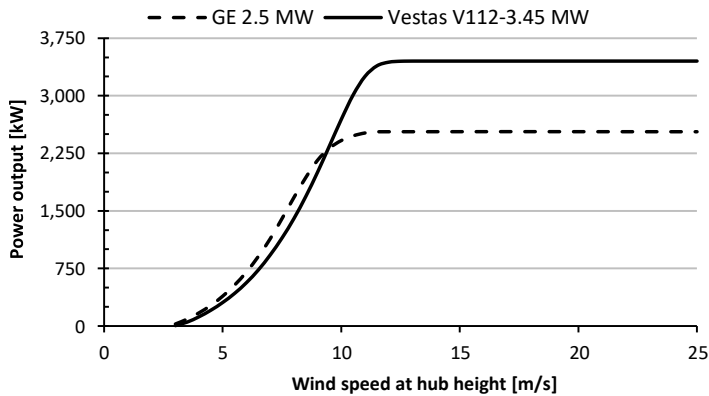


Figure 3: Power curves of considered wind turbines

Investment and O&M cost data for the corresponding countries is taken from (17) and given in Table S.8 and S.9 of the supplementary information. Since installed costs are given, no Lang-factors are required. Labor demand amounts to 87 FTE for each GW of installed wind power capacity (27).

### 3.2. Electricity storage

For the intermittent storage of electric energy, only technologies that are independent of geographic locations will be included in the model, i.e., pumped-hydro storage and compressed-air energy storage are not considered. Fly wheels are excluded due to their high costs and self-discharging rates (44). Therefore, only battery systems are considered. Data for Li-ion, lead and vanadium redox flow (VRF) batteries is taken from Jülch et al. (45) and listed in Table S.10 and S.11 in the supplementary information.

### 3.3. Hydrogen production

Hydrogen is produced in either an alkaline or PEM electrolyzer unit (AEL or PEM-EL). The alkaline electrolyzer is a mature technology with the global installed capacity reaching the MW-scale (46). Contrary, there are still challenges that need to be addresses in order to achieve a large-scale implementation of the PEM-EL, e.g., the reduction of iridium loading due to the low availability of the metal (47). The required electrolyzer capacity in this study reaches the low GW-scale. Currently, most large-scale projects are focused on building electrolyzer units with capacities around 10 – 100 MW (48-50). Therefore, cost data for 100 MW units will be considered and the required capacity will be achieved by numbering up. Specific costs are 400 US-\$<sub>2020</sub>/kW for an AEL and 500 US-\$<sub>2020</sub>/kW for a PEM-EL (51). To estimate the installed costs of the whole electrolyzer unit, a Lang-factor of 1.62 is considered<sup>2</sup> (52). For O&M costs, the same assumptions as in Schnülle et al. are used (11). Furthermore, Schnülle et al. have been shown that water costs have only a small impact on the final hydrogen costs. Therefore, water costs are neglected in this study. For the whole

<sup>2</sup> The „Lang“ factor for the electrolyzer is significantly smaller than the previously mentioned value of 5. The value of 5 is an empirical value mainly derived from apparatus and machines used in chemical fluid processing plants. Therefore, it is adapted for an electrochemical unit.

production plant, a load flexibility of 0 – 100 % is considered. This flexibility does not apply to a single electrolyzer but is assumed to apply to the entire system as several units will be operated in parallel. For simplicity reasons, the efficiency is considered to be independent of the load and no electricity demand is considered for stand-by. The AEL requires 51.9 kWh/kg<sub>H<sub>2</sub></sub> and the PEM-EL 54.3 kWh/kg<sub>H<sub>2</sub></sub>. Since the electrolysis is a highly automated process, the required labor demand is rather low and no data from literature could be obtained. It is assumed that two people per shift are required for every 100 MW of installed electrolyzer capacity. Regarding the sensitivity analysis, Vartiainen gives different values for utility-scale CAPEX for the years 2030 – 2050 with costs decreasing from 240 €/kW<sub>el</sub> to 80 €/kW<sub>el</sub> (12). The value of 80 €/kW<sub>el</sub> is considered to be too optimistic in the authors opinion. Therefore, the system costs of 160 €/kW<sub>el</sub> with an efficiency of 48 kWh/kg<sub>H<sub>2</sub></sub> are chosen as a very optimistic scenario for the sensitivity analysis S2 and S3. Input data for the hydrogen production is summarized in table S.12 and S.13 of the supplementary information.

### **3.4. Hydrogen compression and storage**

Compressed hydrogen storage at a level of 250 bar is considered for the intermittent hydrogen storage. Higher storage pressures are not beneficial from an economic point of view (53). In the required compression step, a maximum pressure ratio of 3 is assumed per stage (54). For simplicity reasons, the pressure after the compressor step is always 250 bar. Hydrogen losses of 0.8 % are considered in the compression step due to leakage from the sealings (55). Cost data for the compressor is taken from literature for the size of a 4'000 kW reciprocating compressor (54). This size has been chosen as a compromise between economy of scale and redundancy. The procurement costs for the storage containers are 700 \$<sub>2020</sub>/kg<sub>H<sub>2</sub></sub> (56). The Lang-factor for the storage is assumed to be 2 (57). A labor demand of 1 person per shift and 5 t of hydrogen storage capacity is assumed for surveillance. Input data for hydrogen compression and storage is summarized in Table S.14 and S.15 of the supplementary information.

## 4. Results and Discussion

A TEA of a hydrogen production plant for several locations was conducted with the goal to minimize the levelized costs of hydrogen for every considered case. The individual technical aspects as well as costs for every unit operation of the plant were estimated with data from the given references. This section gives an overview over the key findings. Detailed results can be found in the supplementary information.

### 4.1. Technical evaluation

The aim of generating large amounts of hydrogen is the transformation of renewable electric energy into a versatile chemical that can be utilized elsewhere. Therefore, it is relevant to know how the renewable energy can be used the most efficient way. Depending on the different climatic conditions and the predefined cases from Table 2 the required installation capacities change, also leading to different utilization factors of the corresponding units. Figure 4 shows the required installed capacities of the RE sources of the plant layout with the lowest LCOH<sub>2</sub> for the different locations and the defined cases. The dashed grey horizontal line indicates the power demand of a constantly running alkaline electrolyzer that generates the required hydrogen mass flow of 25.74 t/h.

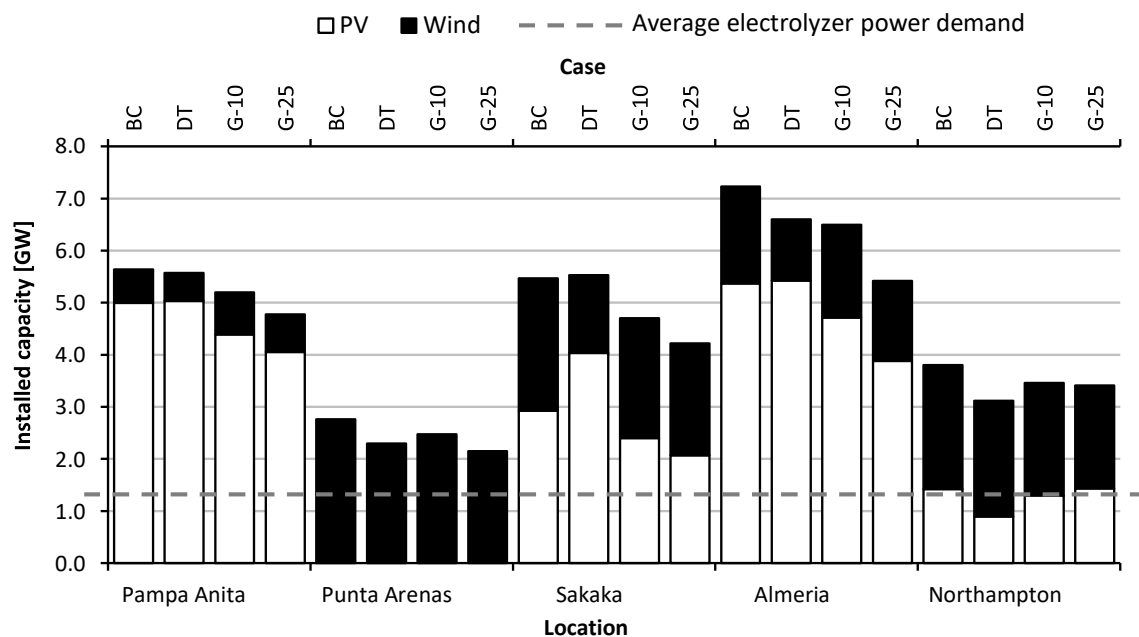


Figure 4: Installed PV and wind farm capacity for the different locations and cases

It can be seen how the tool adapts the most economic plant layout to the different climatic conditions and cases. While PV is preferred as RE supply for both in Pampa Anita and Almeria, in Punta Arenas and Northampton wind energy is preferred with the former using it exclusively. In every run wind turbine II (adapted on GE 2.5) is the more economic option. The base case is almost always the case with the highest installed capacity of RE generation. Enabling the plant to draw a certain

electric power demand from the grid leads to a decrease of the required capacity of RE generation, while the ratio of installed PV to wind capacity is almost unaffected by this. For the downtime case, the installed capacity decreases in Punta Arenas, Almeria and Northampton compared to the base case while it increases in Sakaka. In Pampa Anita almost no change is observable. Furthermore, in Sakaka it can be seen that the ratio between installed PV and wind capacity changes. Since the installed RE capacity exceeds the size of the electrolyzer in every location, RE has to be curtailed if the RE sources run at full capacity. In Figure 5 the different RE utilization rates for the different cases and locations are shown.

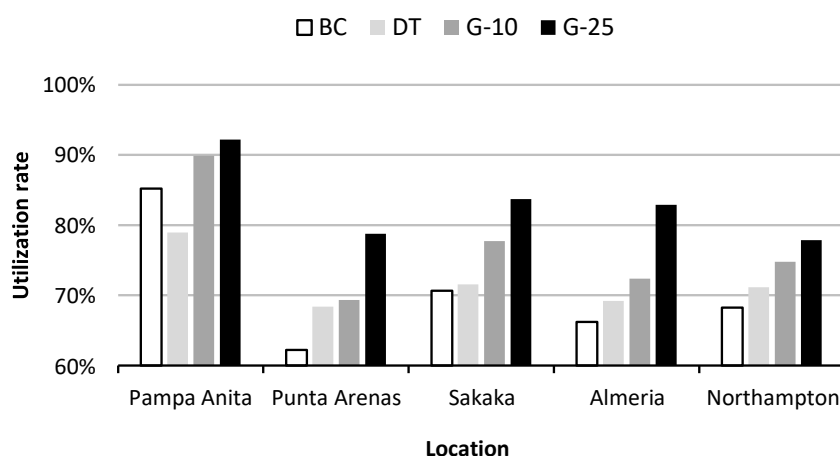


Figure 5: Utilization rate of RE for the different locations and cases

It can be seen that the ratio of utilized RE increases if grid participation is possible. This meets the expectation because the plant doesn't need to be as over-dimensioned as in the base case. Increasing storage capacity and thus increasing the utilization rate in the base case would lead to higher LCOH<sub>2</sub>. Therefore, increasing the utilization rate in the base case is not economically beneficial. Again, for the downtime case no clear trend is observed. The utilization ratio even decreases in Pampa Anita. Since it is the aim to convert RE into hydrogen, it is relevant to know how much grey energy from the grid is used in the G-10 and G-25 cases. The share of used grid energy compared to the total amount of energy used is listed in Table 5. Even in the G-25 case less than 8 % of the used energy is drawn from the grid.

Table 5: Percentage of grid energy used for hydrogen production

Location	G-10	G-25
Pampa Anita	2.0%	7.6%
Punta Arenas	0.4%	1.7%
Sakaka	0.7%	3.3%
Almeria	0.8%	4.8%
Northampton	0.5%	1.7%

Electricity storage was not considered by the tool in every location for every case. The reason behind this will be discussed in subchapter 4.3. Furthermore, only the alkaline electrolysis is used in every evaluation since it is more economic. The installed electrolyzer capacity is shown in Figure 6. As in Figure 4, the dashed grey horizontal line indicates the power demand of a constantly running alkaline electrolyzer that generates the required hydrogen mass flow of 25.74 t/h. The actual electrolyzer capacity has to be over-dimensioned for times where the electrolyzer is idle. Pampa Anita and Almeria, both locations with a high share of PV for installed RE capacity, have larger electrolyzer capacities than locations that focus on wind energy. This also meets the expectation because over-production and storage are required to supply the downstream plant with hydrogen during the night. While the electrolyzer in Punta Arenas is only oversized by 38 % for the base case, this value rises to 168 % in Pampa Anita.

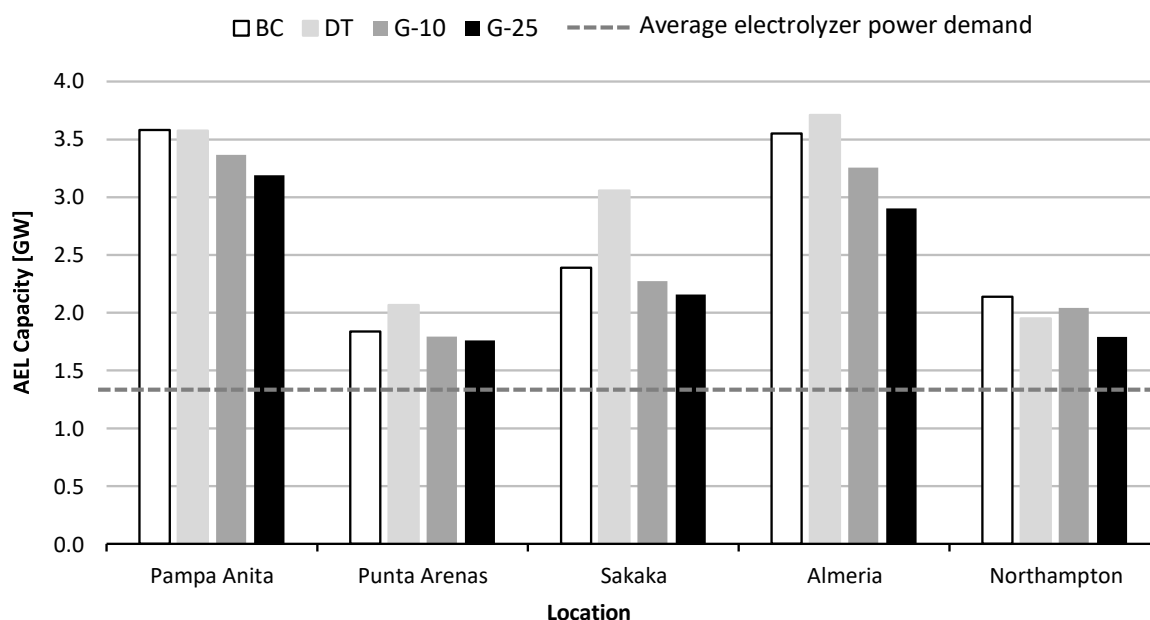


Figure 6: Installed electrolyzer capacity for the different locations and cases

A reduction of electrolyzer capacity can be seen for all cases with grid participation and is more prominent for locations with a high installed PV capacity, especially in Almeria where the electrolyzer capacity is 0.65 GW (-18.3 %) lower in the G-25 case than the base case. The installed electrolyzer capacity in Punta Arenas is already close to the minimum required size, so the reduction potential is also low compared to other locations. The utilization ratio of the electrolyzers is shown in Figure 7. Since the produced amount of hydrogen is the same for all locations, the correlation between a higher installed capacity and a lower utilization ratio is expected.

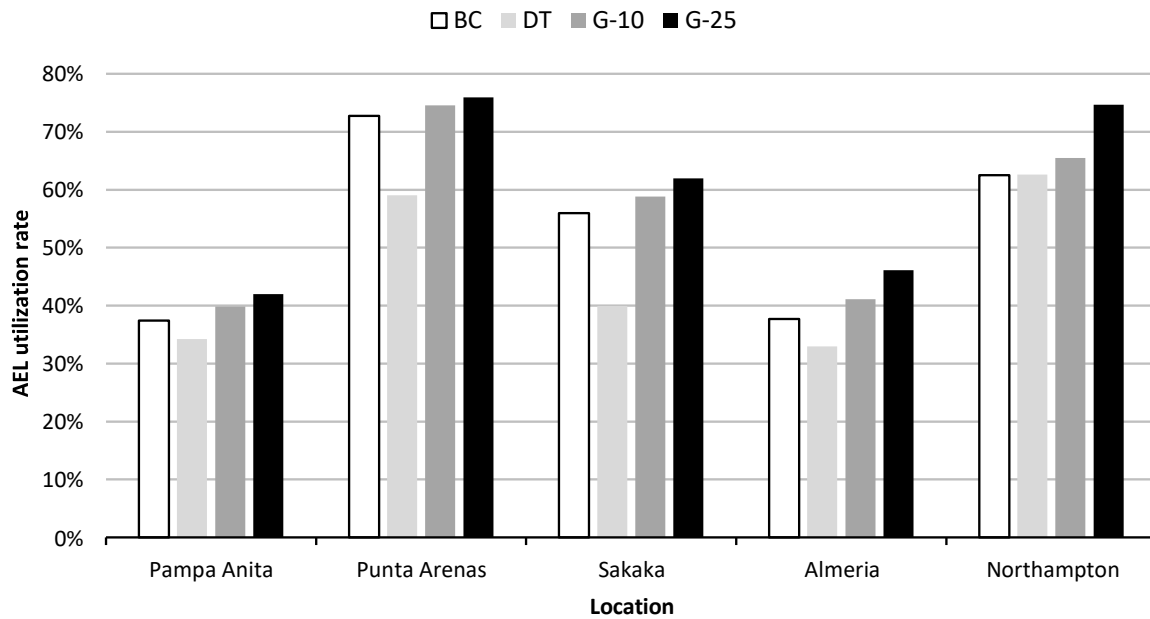


Figure 7: Utilization ratio of the electrolyzers for the different locations and cases

In order to overcome the intermittency of the RE supply and therefore the hydrogen production, compressed hydrogen storage was chosen for the most economic plant layout in every evaluation. The required storage capacity is shown in Figure 8. On the right axis the maximum duration is given, how long the storage tanks could supply the downstream processing plant with hydrogen. If the storage tanks were fully loaded and the only hydrogen source for the downstream plant.

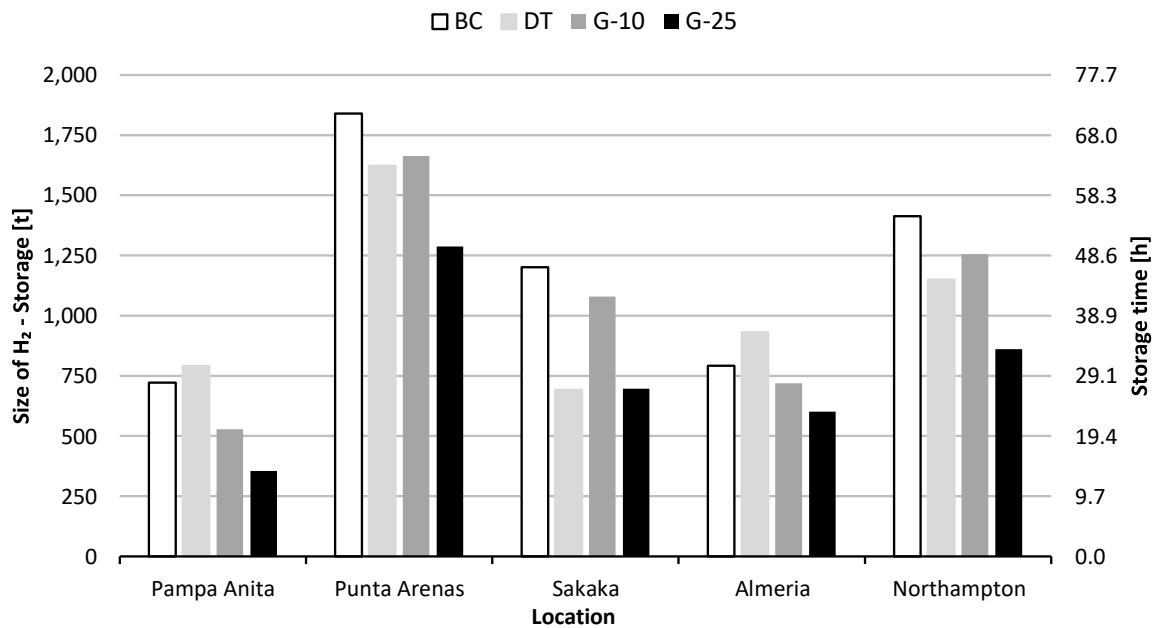


Figure 8: Required compressed hydrogen storage capacity for the different locations and cases

It can be seen that locations with a high amount of installed PV capacity tend to require a smaller storage capacity. Especially in Pampa Anita the required capacity is rather small and can even be halved by enabling the usage of grid energy. Punta Arenas requires the largest storage capacity. This might be because it only relies on wind energy as RE source and that the option is more economic than installing additional PV farms. The size of the storage capacity is not the only decisive factor. Similar to the electric energy storage the maximum charging rate is also relevant. This value is a result from the model and is determined by the amount of installed compressor capacity. The results are depicted in Figure 9. Surprisingly, the required capacity of the compressor increases for the cases with grid assistance. Furthermore, the locations with a small required storage capacity have a higher compression capacity and thus, a higher “charging” rate for the compressed hydrogen storage. For locations with a high share of RE supplied from PV farms, the mass flow to the storage facilities can be up to twice as high as the mass flow to the downstream processing plant. This is indicated by the right axis in Figure 9. The large required compression capacities for these locations are in accordance with the results from Figure 6 where the required capacities of the electrolyzers are shown. In peak production times, the hydrogen produced from a strongly over-dimensioned electrolyzer also has to be processed in a certain way. A detailed analysis on the utilization of the storage devices can be found in chapter S.4 where the amount of hydrogen stored over the course of the year is depicted in a sorted and descending order.

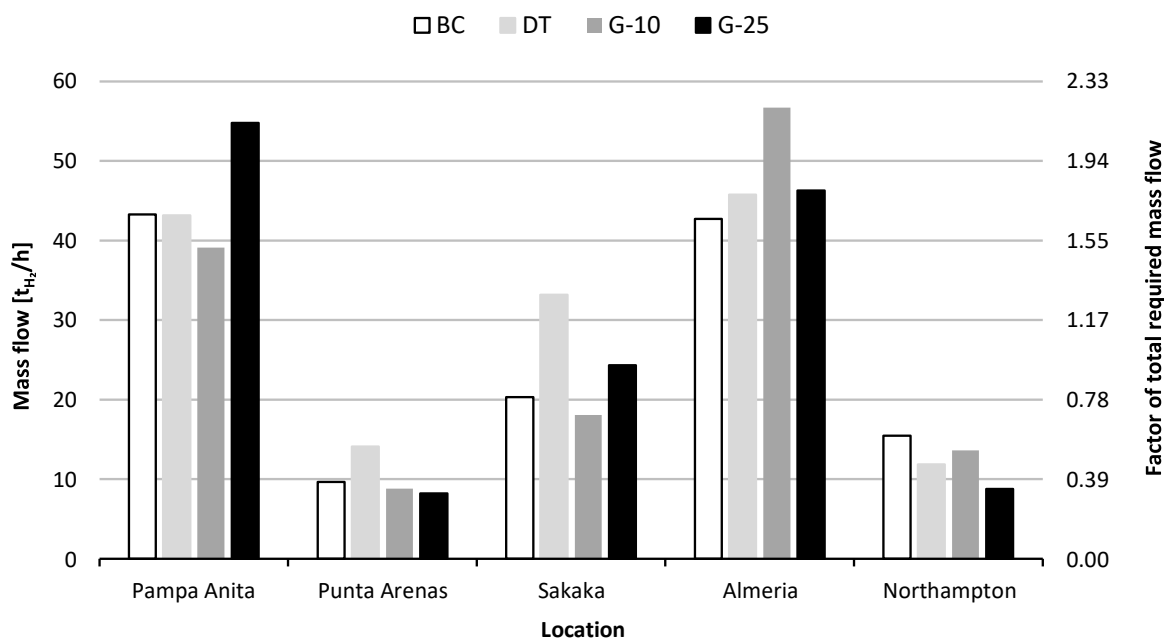


Figure 9: Installed compression capacity for the different locations and cases

## 4.2. Economic evaluation

For the economic evaluation the FCI and the resulting depreciation costs as well as OPEX are estimated. Based on those, the levelized costs of hydrogen are given in €<sub>2020</sub>/kg<sub>H<sub>2</sub></sub>. Figure 10 shows the absolute and specific FCI for the different locations and pathways.



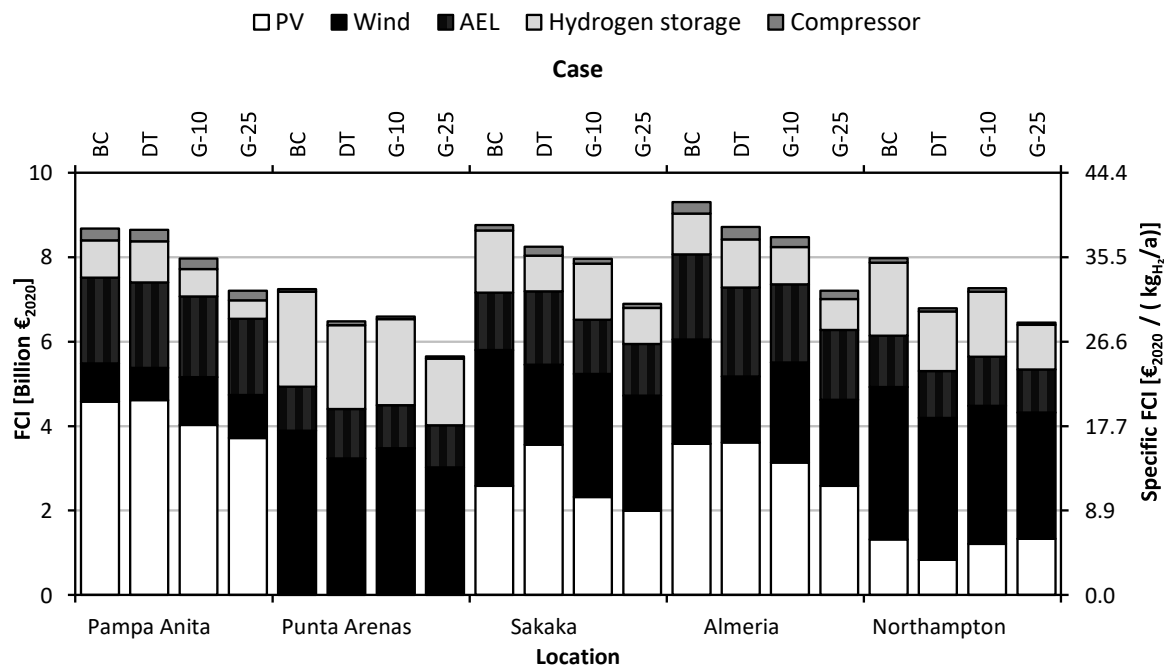


Figure 10: FCI for the hydrogen production plant for the different locations and cases

The specific values on the right axis of Figure 10 are based on the annual amount of 225'500 tons of hydrogen. In order to produce hydrogen in this scale, the required investments are roughly in the range of 7 – 9 billion € for the base case. Since this case requires the highest installed capacities for the different unit operations, it also has the highest FCI for every location. In most locations the RE supply is clearly the most dominant cost contributor of the FCI. In Punta Arenas the RE supply still accounts for roughly half of the FCI. The share of hydrogen storage is also very high due to the aforementioned reasons. With the possibility to use electric energy from the grid, the FCI is reduced in every location. For the G-10 case, the reduction amounts to 8.1 – 9.1% for the different locations and reaches 16.9 – 22.4 % in the G-25 case. The levelized costs of hydrogen are shown in Figure 11.

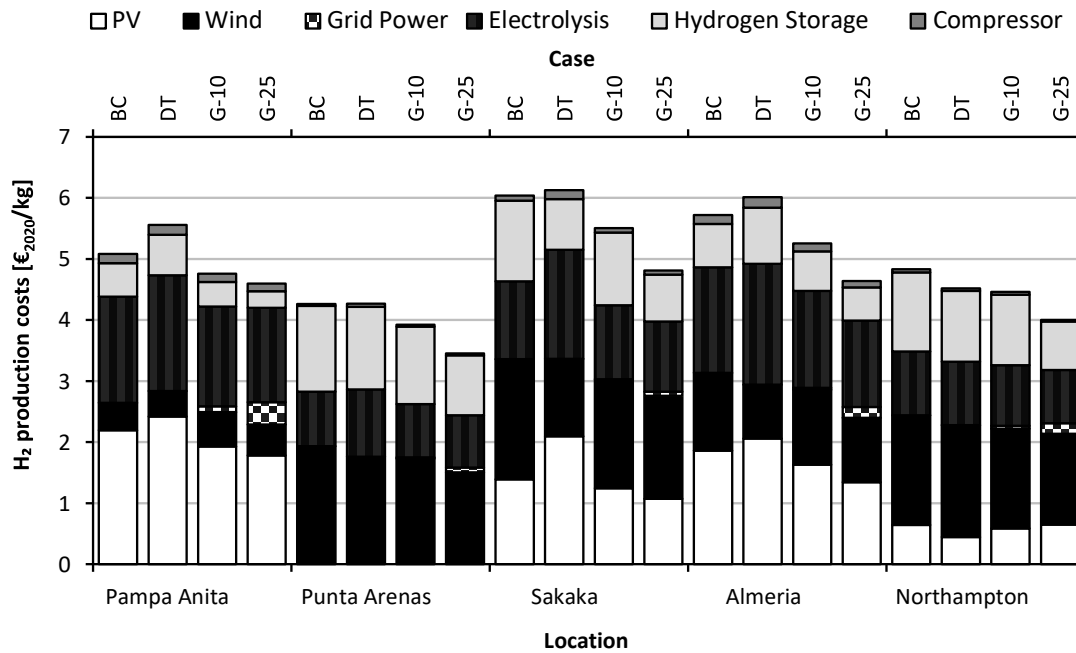


Figure 11: LCOH<sub>2</sub> for the different locations and cases

Except for the location of Northampton, the DT case is more expensive than the base case. Especially for Pampa Anita the consideration of a downtime has a negative effect on the LCOH<sub>2</sub>. Therefore, this case is not further considered in the sensitivity analysis. The effect of grid participation reduces the LCOH<sub>2</sub> in every location. The costs of electricity from the grid are almost negligible for the G-10 case in every location. Only for the G-25 case in Pampa Anita they are roughly as relevant as the costs for hydrogen storage and compression. In both cases, G-10 and G-25, the smaller installed capacity, as depicted in Figure 4, outweighs the cost of electricity from the grid and causes a reduction of the LCOH<sub>2</sub>. In general, the LCOH<sub>2</sub> are lowest in Punta Arenas with 3.45 €/kg<sub>H<sub>2</sub></sub> in the G-25 case as the most economic option.

The results of the sensitivity analysis introduced in Table 2 are depicted in Figure 12. In the analysis, the LCOH<sub>2</sub> retrieved with current cost (CC) data are compared with LCOH<sub>2</sub> retrieved considering perspective costs for PV (S1), the electrolyzer (S2) and for both (S3). The total height of the individual columns corresponds to the current cost scenario shown in Figure 11. The cost altering effect is shown for every individual sensitivity. To evaluate the cost reduction potential, the black colored part of the column plus the corresponding boxes above the part have to be considered. It can be seen for Punta Arenas that no cost reduction from CC to S1 and from S2 to S3 is visible in the diagram. The location relies only on wind power in every evaluation and therefore, the current LCOH<sub>2</sub> are equal to LCOH<sub>2</sub> of S1. The same applies to the LCOH<sub>2</sub> of S2 and S3, respectively. The reduction of electrolyzer costs in S2 has a stronger influence on the LCOH<sub>2</sub> than lower costs for PV in S1 for every case in every location. It is most prominent in Almeria followed by Pampa Anita. This is in accordance with the results shown in Figure 6 since both locations have the largest installed electrolyzer capacity and the lowest utilization rate of the electrolyzer. In the S3 sensitivity it can be

seen that all LCOH<sub>2</sub> are below 4 €/kg<sub>H<sub>2</sub></sub> with most values in the range between 3 – 4 €/kg<sub>H<sub>2</sub></sub>. Only in Chile and Northampton in the G-25 case the costs reach values below 3 €/kg<sub>H<sub>2</sub></sub> with 2.50 €/kg<sub>H<sub>2</sub></sub> in Pampa Anita for the case of G-25 as the most economic option of S3. One aspect that applies for every sensitivity is a change in the merit order of the most economic option, e.g., when future costs for PV and the electrolyzer are considered (S3), hydrogen can be produced more economical in Pampa Anita than in Punta Arenas. This is not the case using current costs or in the S2 evaluation. Detailed results of the sensitivity can be found in chapter S.4 of the supplementary information.

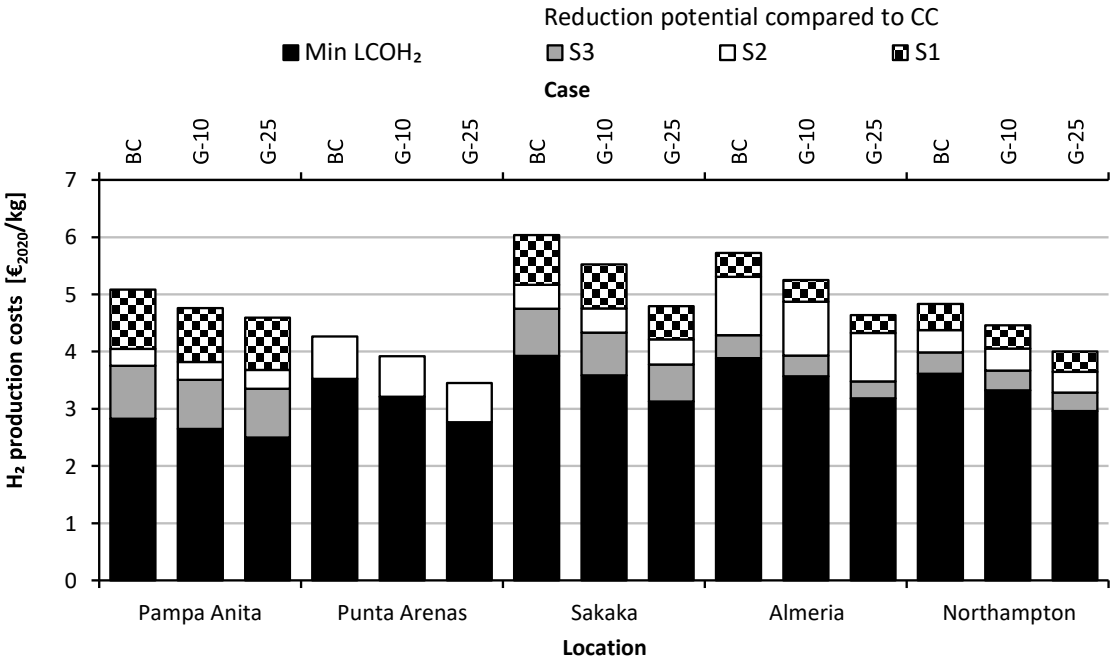


Figure 12: Reduction potential of different sensitivities on the LCOH<sub>2</sub>

### 4.3. Discussion

With the developed tool the layout of a plant producing hydrogen from RE and grid electricity can be determined. It is shown that with the current technological progress and the conditions of the base case,  $\text{LCOH}_2$  between 4 – 6  $\text{€}_{2020}/\text{kg}$  are feasible. One major finding of this study is the advantage that grid assistance has appreciable impact on the technical and economic key performance indicators. The grid connection leads to lower installed capacities of the unit operations while increasing their utilization rate. Especially for the G-25 case in Punta Arenas, where only 1.7 % of the total energy is drawn from the grid, the  $\text{LCOH}_2$  are reduced by almost 20 % compared to the base case. Therefore, when such a plant is built in the future it should be expected to interact with the local grid to bridge times with low local RE supply and even sell excess energy to the grid instead of curtailing it. In subchapter 4.1 it is stated that no electricity storage is used in the evaluations. The aspect that electricity storage is not economic compared to hydrogen storage has already been explained by Mallapragada (10). For a comparison it has to be considered if it is more economic to store the electric energy to produce one kg of hydrogen or storing the actual produced hydrogen. Even with perspective data from Jülich, the cheapest specific costs prediction is 190  $\text{€}_{2015}/\text{kWh}_e$  for storing electric energy (45). This corresponds to 6'333  $\text{€}_{2015}/\text{kg}_{\text{H}_2}$  with the LHV of 33.33  $\text{kWh}/\text{kg}_{\text{H}_2}$ , so even without considering the efficiency losses from the electrolyzer, it is 10 times more expensive than the specific costs for storing compressed hydrogen with roughly 613  $\text{€}_{2020}/\text{kg}_{\text{H}_2}$ , (neglecting the different reference years). Therefore, focusing on compressed hydrogen storage to achieve a constant hydrogen supply is the more economic option.

The results of the base case from this study confirm the outcomes of previous studies for the installation year 2020. Schnülle et al. received minimum  $\text{LCOH}_2$  of 4.33  $\text{€}_{2020}/\text{kg}$  with onshore wind turbines after their remuneration period (11). While Mallapragada estimated  $\text{LCOH}_2$  of 2.5  $\text{\$/kg}$  for 2030 with perspective cost data and a salt cavern for intermediate hydrogen storage (10). This is in accordance with the results from the sensitivity analysis shown in Figure 12, especially, if the given accuracy of the applied cost estimation and the influence of the different locations are considered.

Several aspects have to be acknowledged that influence the presented results. One aspect is the stiff requirement of a constant mass flow over the whole period of time. The evaluated hydrogen production plant is supplying an undefined downstream plant. For this study, only the hydrogen production plant was considered to be flexible which corresponds to a scenario with maximum  $\text{LCOH}_2$ . If a range is required instead of a fixed value, e.g., a mass flow of 25.74  $\text{t/h} \pm 15\%$  (21.9 – 29.6  $\text{t/h}$ ) the required storage demand and subsequently the  $\text{LCOH}_2$  could be reduced. Another aspect is the weighted average cost of capital (WACC) since the gained  $\text{LCOH}_2$  are dominated by the depreciation of the FCI. With the given mass flow, a WACC of 5 % and 20 years as depreciation time, 0.134  $\text{€}/\text{kg}_{\text{H}_2}$  per billion  $\text{€}$  investment account for the cost of capital. This value increases to 0.213  $\text{€}/\text{kg}_{\text{H}_2}$  per billion  $\text{€}$  investment for the WACC of 7.5 % in Saudi Arabia. Recently, an increase of the inflation rate was observed accompanied with insecurities regarding the interest rate policies. This could also influence the WACC of the different countries and thus influence the

merit order of a ranking based solely on LCOH<sub>2</sub>. With the required FCIs from Figure 10 that are in the range between 5.5 and 9 billion €, the share of costs for capital can reach values of up to 25 % from the LCOH<sub>2</sub>. Other uncertainties in the calculation originate from simplifications, e.g.: in a future study it could be evaluated whether the costs for water can really be neglected for locations like Pampa Anita or Sakaka since the hydrogen mass flow corresponds to a water flow of 2'300 t/h. Furthermore, transmission and transformation losses of electric energy are neglected and there is no difference considered in the form of electricity (AC or DC). However, the simplifications do not substantially influence the results of the mathematical model and how the interaction with the electric grid reduces the LCOH<sub>2</sub>. One of the most important input variables are the weather data, for which the year 2019 is used as the reference year. Furthermore, as stated in section 2.2 the mathematical model has "perfect foresight" of the used weather data while an operator of a real plant can only rely on weather forecasts and seasonable changes. Another aspect that has not been considered regarding the usage of wind energy is the influence of turbulent weather conditions like wind gusts. In every case wind turbine II is more economic which might change when actual cost data for the wind turbines is used or if other aspects limit the selection, e.g., regarding wind classes and allowed turbulences. These aspects could be addressed by further research.

The EU has set the goal to produce green hydrogen with costs lower than 1.80 €/kg by the year 2030 (58). The results of Figure 12 indicate that there are still aspects that need to be addressed to reach this goal. But it seems reachable since the lowest costs amount to 2.50 €<sub>2020</sub>/kg<sub>H<sub>2</sub></sub> in Pampa Anita in the G-25 case and the S3 sensitivity. By considering additional technical progress for the intermediate hydrogen storage, a reduction in the WACC and softening the requirement of the constant mass flow, the goal of 1.80 €/kg can be achieved. However, the costs from Vartiainen, 0.30 - 0.84 €/kg for the year 2050, seem to be very ambitious but cannot be ruled out if the costs for PV and the electrolyzer will develop in the presented manner of their study (12). The same challenge applies to the target of \$1/ kg<sub>H<sub>2</sub></sub> that has slightly higher costs but is supposed to be reached by the year 2030 (59).

Technical progress can be expected for every unit of the plant layout, e.g., bifacial solar cells or the consideration of a tracking system which could decrease the costs of solar electricity. By implementing new data to the mathematical model, the tool can automatically determine the improvements and estimate the adapted LCOH<sub>2</sub>.

## 5. Conclusion

In this study a method is described to automatically retrieve the layout of a cost optimized hydrogen production plant for different locations around the world. The developed tool is able to determine the cost-optimized size of RE production capacity, electrolyzer, compressor and H<sub>2</sub> storage capacity for a constant supply of 25.74 t/h to a downstream plant (225'500 t/a). The operation of such a plant in an island mode is neither realistic nor beneficial, since the plant has to be drastically over dimensioned in order to supply hydrogen 100 % of the time. A certain amount of grid assistance was able to reduce the required installed capacities of the individual units and thus also reduce the LCOH<sub>2</sub>. Technical and economic aspects of the different geographic locations have been presented and can be adapted for cost estimations of different scenarios or for further future costs developments. To the knowledge of the authors no study has been published where the cost calculation is described as detailed and reproducible and the influence of grid assistance on the plant layout has been discussed.

Utilizing current knowledge about the technical progress and best practice chemical process cost engineering methodology the lowest achievable current costs for the considered locations are 3.45 €<sub>2020</sub>/kg<sub>H<sub>2</sub></sub> in Punta Arenas in the G-25 case. Future costs in the range of 2.50 – 4 €<sub>2020</sub>/kg<sub>H<sub>2</sub></sub> can be expected for all evaluated locations just by considering progress for PV panels and the alkaline electrolyzer, as shown in Figure 12 for the sensitivity S3. Based on the results shown in this study, a life cycle assessment of such a hydrogen production plant could evaluate the impacts of grid participation. Some questions to be answered are: How “green” is the produced hydrogen and do the reduced installed RE capacities outweigh the share of grey energy from the grid?

Imprecisions of the presented methodology have to be reduced in future research to increase the resilience of the study results. Lang-factors should be validated for each unit individually, especially regarding the electrolyzer where a lot of studies often neglect installation costs. Future research could also implement additional technologies. In this study only one-axis and non-tracking PV panels have been considered and no geographically bound units like a salt-cavern were evaluated. Furthermore, softening the strict requirement of the constant mass flow might be provided by actual H<sub>2</sub> consumers. Apart from considering aspects that might further decrease the LCOH<sub>2</sub> it will be relevant to understand the future hydrogen consumer's perspective and how a customer wants to achieve its CO<sub>2</sub> abatement goals with the least costs and the highest process and delivery safety.

## **6. Declaration of competing interest**

The authors declare that they have no known competing financial interests or personal relationships that could have appeared to influence the work reported in this paper.

## Abbreviations

AEL	Alkaline electrolyzer
BC	base case
CAPEX	Capital expenditures
CC	current costs
DT	downtime (referring to downtime case)
FCI	Fixed capital investment
FTE	Full time equivalent
GHG	Greenhouse gases
LCOE	Levelized cost of electricity
LCOH <sub>2</sub>	Levelized cost of hydrogen
OPEX	operating expenditures
O&M	Operating and maintenance costs
PEM-EL	Proton exchange membrane – electrolyzer
PtX	Power to X
PV	photovoltaic (referring to solar energy)
RE	Renewable energy
TEA	techno-economic assessment
WACC	Weighted average cost of capital



## Bibliography – Paper

1. Gielen D, Gorini R, Leme R, Prakash G, Wagner N, Janeiro L, et al. World Energy Transitions Outlook: 1.5° C Pathway. 2021.
2. Sognaes I, Gambhir A, van de Ven D-J, Nikas A, Anger-Kraavi A, Bui H, et al. A multi-model analysis of long-term emissions and warming implications of current mitigation efforts. Nature Climate Change. 2021.
3. Casey J. Siemens begins work on 8.75 MW green hydrogen plant in Germany: Power Technology; 2021 [Available from: <https://www.power-technology.com/news/siemens-begins-work-on-8-75mw-green-hydrogen-plant-in-germany/>].
4. Morison R. Giant offshore Irish Wind Farm planned for Green Hydrogen: Bloomberg L.P.; 2021 [Available from: <https://www.bloomberg.com/news/articles/2021-11-22/giant-offshore-wind-farm-planned-in-ireland-for-green-hydrogen>].
5. Paddison L. Oman plans to build world's largest green hydrogen plant: The Guardian; 2021 [Available from: <https://www.theguardian.com/world/2021/may/27/oman-plans-to-build-worlds-largest-green-hydrogen-plant>].
6. (BMWi) BfWuE. Die Nationale Wasserstoffstrategie. Die Bundesregierung; 2020.
7. Knipperts A. Neue Energie für globale Partnerschaften? 2021. Available from: <https://bdi.eu/publikation/news/neue-energie-fuer-globale-partnerschaften-wasserstoff-energie-h2/>.
8. Loewert M, Pfeifer PJ. Dynamically Operated Fischer-Tropsch Synthesis in PtL-Part 1: System Response on Intermittent Feed. 2020;4(2):21.
9. Klein H, Fritsch P, Haider P, Kender R, Rößler F, Rehfeldt S, et al. Flexible Operation of Air Separation Units 2021;8(4):357-74.
10. Mallapragada DS, Gençer E, Insinger P, Keith DW, O'Sullivan FM. Can Industrial-Scale Solar Hydrogen Supplied from Commodity Technologies Be Cost Competitive by 2030? Cell Reports Physical Science. 2020;1(9):100174.
11. Schnuelle C, Wassermann T, Fuhrlaender D, Zondervan E. Dynamic hydrogen production from PV & wind direct electricity supply – Modeling and techno-economic assessment. International Journal of Hydrogen Energy. 2020;45(55):29938-52.
12. Vartiainen E, Breyer C, Moser D, Román Medina E, Busto C, Masson G, et al. True Cost of Solar Hydrogen. 2021;n/a(n/a):2100487.
13. Ausfelder F, Dura HE, Cadavid Isaza A, de la Rua C, Gawlick J, Hamacher T. 3. Roadmap des Kopernikus-Projektes P2X Phase II. 2021.
14. Pfennig M, Bonin M, Gerhardt NJZJ. „PtX-Atlas: Weltweite Potenziale für die Erzeugung von grünem Wasserstoff und klimaneutralen synthetischen Kraft- und Brennstoffen“, Teilbericht im Rahmen des Projektes: DeV-KopSys, Mai 2021. 2021;27.
15. Schemme S, Breuer JL, Köller M, Meschede S, Walman F, Samsun RC, et al. H<sub>2</sub>-based synthetic fuels: A techno-economic comparison of alcohol, ether and hydrocarbon production. International Journal of Hydrogen Energy. 2020;45(8):5395-414.
16. Raab M, Maier S, Dietrich R-U. Comparative techno-economic assessment of a large-scale hydrogen transport via liquid transport media. International Journal of Hydrogen Energy. 2021;46(21):11956-68.
17. IRENA. Renewable Power Generation Costs in 2020. 2021.
18. Albrecht FG, König DH, Baucks N, Dietrich R-U. A standardized methodology for the techno-economic evaluation of alternative fuels – A case study. Fuel. 2017;194:511-26.
19. Peters MS, Timmerhaus KD, West RE. Plant design and economics for chemical engineers: McGraw-Hill New York; 2003.
20. Lang H. Cost relationships in preliminary cost estimation. Chem Eng. 1947;54(10):117-21.

21. Gurobi Optimization L. Gurobi Optimizer Reference Manual. 2021.
22. Lu X, McElroy MB, Kiviluoma J. Global potential for wind-generated electricity. 2009;106(27):10933-8.
23. ESMAP S, WB I. Global Solar Atlas Glob. Sol. Atlas. 2019.
24. Gräve P. Baubeginn für weltweit erste integrierte kommerzielle Anlage zur Herstellung von eFuels: Porsche; 2021 [Available from: <https://newsroom.porsche.com/de/2021/unternehmen/porsche-baubeginn-kommerzielle-anlage-herstellung-co2-neutrale-kraftstoffe-chile-25681.html>].
25. Power-Technology. Sakaka Photovoltaic Solar Project 2021 [Available from: <https://www.power-technology.com/projects/sakaka-photovoltaic-solar-project/>].
26. DLR-SF. CIEMAT Plataforma Solar de Almería - Europe's biggest Test Center for Concentrating Solar Power (CSP) [Available from: [https://www.dlr.de/sf/de/desktopdefault.aspx/tabid-7176/11942\\_read-28189/](https://www.dlr.de/sf/de/desktopdefault.aspx/tabid-7176/11942_read-28189/)].
27. Chapman AJ, Fraser T, Itaoka K. Hydrogen import pathway comparison framework incorporating cost and social preference: Case studies from Australia to Japan. Int J Energy Res. 2017;41(14):2374-91.
28. Chinchilla M, Santos-Martín D, Carpintero-Rentería M, Lemon S. Worldwide annual optimum tilt angle model for solar collectors and photovoltaic systems in the absence of site meteorological data. Applied Energy. 2021;281:116056.
29. Statista. Average market price of electricity in Chile from January 2019 to October 2021 2021 [Available from: <https://www.statista.com/statistics/1029737/chile-electricity-average-m/>].
30. ExchangeRates. Euro to Chilean Peso Spot Exchange Rates for 2019 2021 [Available from: <https://www.exchangerates.org.uk/EUR-CLP-spot-exchange-rates-history-2019.html>].
31. SaudiElectricityCompany. Tariffs & Connection Fees 2022 [Available from: <https://www.se.com.sa/en-us/customers/Pages/TariffRates.aspx>].
32. ExchangeRates. Euro to Saudi Riyal Spot Exchange Rates for 2020 2021 [Available from: <https://www.exchangerates.org.uk/EUR-SAR-spot-exchange-rates-history-2020.html>].
33. Statista. Prices of electricity for industry in Spain from 2008 to 2020 2022 [Available from: <https://www.statista.com/statistics/595813/electricity-industry-price-spain/>].
34. FCH. Fuel Cells and Hydrogen Joint Undertaking (FCH 2 JU). 2018.
35. ExchangeRates. Euro to Australian Dollar Spot Exchange Rates for 2020 2021 [Available from: <https://www.exchangerates.org.uk/EUR-AUD-spot-exchange-rates-history-2020.html>].
36. Pfenninger S, Staffell I. Long-term patterns of European PV output using 30 years of validated hourly reanalysis and satellite data. Energy. 2016;114:1251-65.
37. Staffell I, Pfenninger S. Renewables. ninja. URL: <https://www.renewables.ninja/> (visited on 10/11/2021); 2021.
38. Staffell I, Pfenninger S. Using bias-corrected reanalysis to simulate current and future wind power output. Energy. 2016;114:1224-39.
39. Xu Z, Xu X, Cui C, Huang H. A new uniformity coefficient parameter for the quantitative characterization of a textured wafer surface and its relationship with the photovoltaic conversion efficiency of monocrystalline silicon cells. Solar Energy. 2019;191:210-8.
40. Hsu SA, Meindl EA, Gilhousen DB. Determining the Power-Law Wind-Profile Exponent under Near-Neutral Stability Conditions at Sea %J Journal of Applied Meteorology and Climatology. 1994;33(6):757-65.
41. Vestas. V112-3.45 MW® 2021 [Available from: <https://www.vestas.com/en/products/4-mw-platform/V112-3-45-MW>].
42. models Wt. Vestas V112-3.45 2021 [Available from: <https://www.wind-turbine-models.com/turbines/1247-vestas-v112-3.45>].

43. models Wt. GE General Electric GE 2.5 - 120 2021 [Available from: <https://www.wind-turbine-models.com/turbines/310-ge-general-electric-ge-2.5-120>].
44. Dhabi IREAJRA. Electricity storage and renewables: Costs and markets to 2030. 2017.
45. Jülch V. Comparison of electricity storage options using levelized cost of storage (LCOS) method. Applied Energy. 2016;183:1594-606.
46. Shiva Kumar S, Himabindu V. Hydrogen production by PEM water electrolysis – A review. Materials Science for Energy Technologies. 2019;2(3):442-54.
47. Bernt M, Hartig-Weiß A, Tovini MF, El-Sayed HA, Schramm C, Schröter J, et al. Current Challenges in Catalyst Development for PEM Water Electrolyzers. 2020;92(1-2):31-9.
48. Asahi Kasei's "aqualizer" starts producing green hydrogen in Japan. Membrane Technology. 2020;2020(5):2.
49. Radowitz B. Linde to build 'world's largest electrolyser' to produce green hydrogen 2021 21.12.2021. Available from: <https://www.rechargenews.com/transition/linde-to-build-world-s-largest-electrolyser-to-produce-green-hydrogen/2-1-944080>.
50. Shell. Shell starts up Europe's largest PEM green hydrogen electrolyser 2021 21.12.2021. Available from: <https://www.shell.com/media/news-and-media-releases/2021/shell-starts-up-europes-largest-pem-green-hydrogen-electrolyser.html>.
51. IRENA. Green hydrogen cost reduction. 2020.
52. Zauner A, Böhm H, Rosenfeld DC, Tichler RJDAofo, Ares ot-ooR. Innovative large-scale energy storage technologies and Power-to-Gas concepts after optimization. 2019:4315303.
53. Baldwin D, editor Proceedings of DOE Hydrogen Compression, Storage, and Dispensing Cost Reduction Workshop2013: Hexagon Lincoln.
54. Woods DR. Rules of thumb in engineering practice: John Wiley & Sons; 2007.
55. Stolzenburg K, Mubbala RJIdfoeloh, FCH JU. Hydrogen Liquefaction Report. 2013.
56. Abdin Z, Tang C, Liu Y, Catchpole K. Large-scale stationary hydrogen storage via liquid organic hydrogen carriers. iScience. 2021;24(9):102966.
57. Personal communication with expert for hydrogen fuelling stations.
58. EU. Opening keynote by President von der Leyen at the European Hydrogen Week 2021 2021 [Available from: [https://ec.europa.eu/commission/presscorner/detail/en/speech\\_21\\_6421](https://ec.europa.eu/commission/presscorner/detail/en/speech_21_6421)].
59. Collins L. We will reduce the cost of green hydrogen to \$1/kg by 2025', says electrolyser maker chairman: RECHARGE; 2021 [Available from: <https://www.rechargenews.com/energy-transition/producing-green-hydrogen-for-1-kg-is-achievable-in-some-countries-by-2030-woodmac/2-1-1118580>].